Single Cs atoms as collisional probes in a large Rb magneto-optical trap

Claudia Weber, Shincy John, Nicolas Spethmann, Dieter Meschede, and Artur Widera*
Institut für Angewandte Physik, Universität Bonn, Wegelerstr. 8, D-53115 Bonn, Germany
(Received 20 July 2010; published 29 October 2010)

We study cold interspecies collisions of cesium and rubidium in a strongly imbalanced system with single and few Cs atoms. Observation of the single-atom fluorescence dynamics yields insight into light-induced loss mechanisms, while both subsystems can remain in steady state. This significantly simplifies the analysis of the dynamics, as Cs-Cs collisions are effectively absent and the majority component remains unaffected, allowing us to extract a precise value of the Rb-Cs collision parameter. Extending our results to ground-state collisions would allow to use single neutral atoms as coherent probes for larger quantum systems.

DOI: 10.1103/PhysRevA.82.042722 PACS number(s): 34.50.Cx, 34.50.Rk

I. INTRODUCTION

Magneto-optical traps (MOTs) are standard sources for ultracold atoms [1] and are used with multiple species in current experiments [2,3] as a first step toward the creation of, e.g., ultracold heteronuclear molecules [4–6]. In these MOTs, interspecies collisions can lead to dramatic losses compared to the homonuclear case, limiting the density of atoms available and complicating the experimental procedure. For various single-species MOTs the homonuclear loss mechanisms, as well as the corresponding interaction potentials, are well known. However, this knowledge cannot be easily transferred to the heteronuclear case: While the loss mechanisms remain the same, their contributions to the dynamics of the mixed species system can be strongly altered as the internuclear long-range potential is weaker and the short-range interaction dominates. The loss mechanisms include ground-state collisions due to spin exchange and dipolar relaxation interaction as well as light-induced collisions (ground-excited collisions) [1]. The latter processes such as radiative escape and fine-structure changing collisions dominate in traps with near-resonant light [7–9].

The standard methods to extract information about these interspecies interaction processes either consider the loading dynamics of one atomic species in the MOT on presence of another or investigate the change in trapped atom number as one species is removed from the system which was in steady-state previously [10]. In both cases, the simultaneous presence of homonuclear and heteronuclear collisions, both depending on the atomic densities of the respective species, complicate the analysis. In some cases, the losses due to homonuclear collisions are neglected if the corresponding loss rate $\beta_{i(j)}$ is much smaller than the interspecies loss rate $\beta'_{i,j}$ [11].

Here we consider ground-excited collisions in a mixture of cesium (Cs) and rubidium (Rb) [12,13] using a system which combines the advantages of both methods mentioned above. We deduce the loading and loss dynamics of single Cs atoms in the presence of a large Rb MOT, while both subsystems are in steady state. Working with single atoms, the probability for homonuclear Cs-Cs collisions is negligible, simplifying the analysis. In principle, however, our method even allows identifying and counting these rare events. At the same time, the presence of single Cs atoms has no measurable effect on the Rb system.

II. EXPERIMENTAL SETUP

In order to probe cold collisions of the two-species mixtures with a single-atom probe, we trap Rb and Cs simultaneously but in different regimes of atom numbers.

We load single Cs atoms from a low background pressure well below 10^{-11} mbar in a high magnetic field gradient magneto-optical trap (MOT) [14,15]. The relatively high magnetic field gradient of 270 G/cm reduces the loading rate compared to a standard MOT by several orders of magnitude to about 1 atom/s. In order to support a low loading rate the MOT is operated using relatively small MOT beams with a diameter of 1 mm and a total power of 500 μW. The atom number in the MOT is detected by a sensitive fluorescence detection system schematically drawn in Fig. 1. It is based on a high-numerical-aperture objective, with a numerical aperture equal to 0.29, spectral and spatial filters, and an avalanche photodiode operating in a single-photon counting mode (APD-SPCM). In this operating mode, also known as Geiger mode, each detected photon produces a TTL pulse which is accumulated by a counter card. The field of view of the detection setup is about 60 μm in the object plane, which is approximately twice the maximum of the diameter of the high-gradient Cs MOT. We record the fluorescence for up to 4 s, where the photon count rate is binned in time intervals of 20 ms. The detection time is limited by the power dissipation of the quadrupole coils. Then, all cooling laser beams and the magnetic field are switched off for 500 ms so that all atoms escape from the trap. Subsequently, the MOT laser beams are switched on without magnetic field applied, yielding the background light level due to stray light. Typical fluorescence traces are shown in Fig. 2. The discrete fluorescence steps correspond to the loading or loss of one atom [15,16]. The photon count rate per atom is experimentally determined to be 10^4 counts s^{-1}. A corresponding histogram of 200 such traces showing the occurrences of each count rate for the same set of experimental parameters is shown in Fig. 2, where the background rate has been subtracted individually for each trace to eliminate long time drifts. Each peak is attributed to a number of atoms N. In steady state the probability distribution of the detected atom number is described by a Poissonian distribution.

*widera@uni-bonn.de

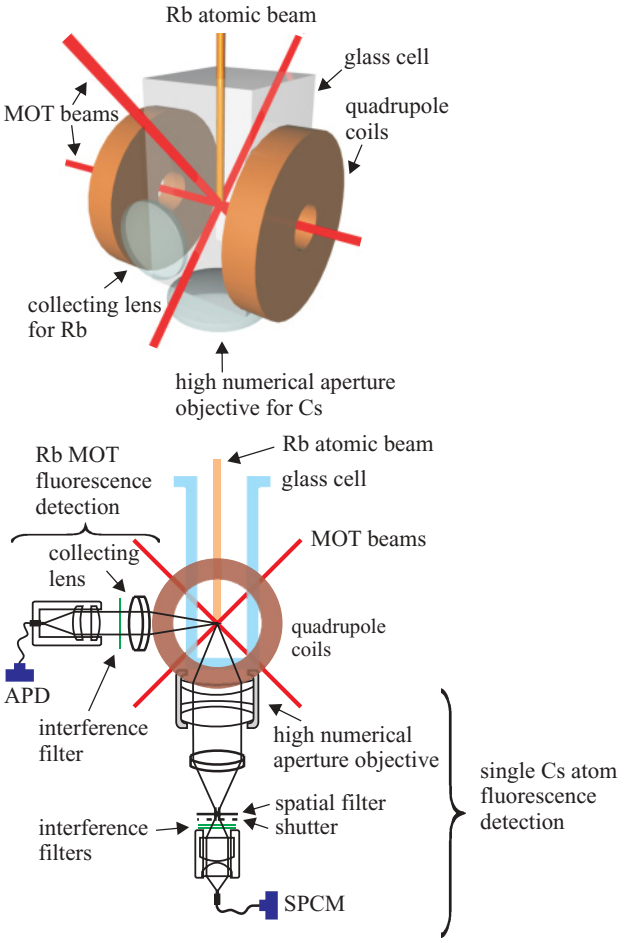

FIG. 1. (Color online) Schematic of the experimental setup to operate and detect a strongly imbalanced two-species MOT. Both MOTs of Rb and Cs are produced at the same position using the same quadrupole coils. The Rb MOT is loaded by an atomic beam (orange) provided by a second vapor pressure MOT, whereas Cs is loaded from the background of the ultrahigh vacuum. The Rb and Cs atom numbers are determined by fluorescence detection setups located at the side and at the bottom of the glass cell, respectively. The Cs fluorescence light collected by a high numerical aperture objective is detected by an APD-SPCM with a quantum efficiency of 42%. To suppress stray light as well as Rb fluorescence and laser light a 300-μm pinhole and two interference filters serve as spatial and spectral filters, respectively. The Rb fluorescence is collected by a lens, spectrally filtered and detected by an APD.

The Rb MOT is superposed to the single Cs MOT by using the same magnetic quadrupole field. Both MOTs can have strongly different atom numbers (up to 3×10^3 atoms for Rb) due to different parameters of the corresponding laser beams. The large wavelength difference of 72 nm between the atomic transitions for Rb (780 nm) and Cs (852 nm) allows adjusting the MOT laser system for each species without affecting the other. For Rb we choose a beam diameter of 16 mm with a power of 100 mW. In addition, the Rb MOT is loaded from an atomic beam originating from a second vapor pressure MOT (see Fig. 1). This atomic beam provides precooled Rb atoms and leads to a local enhancement of the partial Rb background pressure at the MOT position. Thereby the loading rate increases by up to three orders of magnitude compared to the single-atom MOT, resulting in a higher number of stored Rb atoms of up to 3300 atoms. This corresponds to a peak density of 6.5×10^{10} cm^{-3} which is comparable to standard MOT densities. During the experimental sequence an adjustment of the number of Rb atoms trapped is performed by changing the atomic flux of this atom beam without affecting the MOT properties such as position or size. As in the case of Cs the number of Rb atoms is determined by a fluorescence detection system. Due to the much larger atom number of Rb compared to Cs, the corresponding detected fluorescence rate is several orders of magnitude larger for Rb. Therefore, the avalanche photodiode (APD) is operated below the Geiger mode [17], and thus the photon number is directly proportional to the output current, and we obtain direct information about the fluorescence intensity. The absolute number of the Rb atoms is only precise to a factor of 1.3. As schematically drawn in Fig. 1 the determination of the Rb atom number depends on the effective solid angle of detection, on the reflectivity and absorption of the optics used, the fiber coupling efficiency and the responsivity of the APD. The main influence on the uncertainty of the Rb atom number are the two last points due to the nonlinear dependence of the APD responsivity on the operating voltage (40 ± 5) A/W and the estimated fibre coupling efficiency of (60 ± 20) %.

In order to observe interaction between Rb and Cs, we first load Rb atoms in the high-gradient magnetic field MOT for 2.5 s until the Rb atom number is in steady state for a chosen number of Rb atoms. Once this is reached, the Cs MOT-light is switched on and the fluorescence detection signal of Cs is recorded for 3 s. As mentioned above, we then detect the dark count rate and background light level for each trace.

III. ANALYSIS OF CS ATOM DYNAMICS

Cesium fluorescence traces have been recorded for Rb atom numbers in the range between 0 and 3300 Rb atoms. All data are sorted by N_{Rb}, which is binned in steps of 220 Rb atoms, and for each Rb atom number we average over typically 200 traces [18]. An example of two typical traces for three different Rb atom numbers is plotted in Fig. 2. Qualitatively different dynamics of the single Cs atom MOT can already be seen in the single recorded traces. For an almost negligible Rb atom number [Fig. 2(a)], a fast loading of Cs can be observed with only a few loss features, which does not saturate during our observation time. In contrast, only a few loading events can be found for large Rb atom numbers [Fig. 2(c)]. Moreover, loss processes are much more frequent and dominated by single-Cs collisions. All the loading events are followed, within 100 ms, by an atom loss. Within this range of the Rb atom number many traces do not show any event at all.

The corresponding histograms shown in Figs. 2(d)–2(f) mirror this behavior. In Fig. 2(d) for about $N_{\mathrm{Rb}} = 550$ five peaks corresponding to up to four atoms can be observed, whereas in Fig. 2(f) at most one atom is detected [19].

In order to get information about the interspecies collision properties the dynamics of the Cs-MOT is analyzed. In the presence of Rb this dynamics can be described by the rate

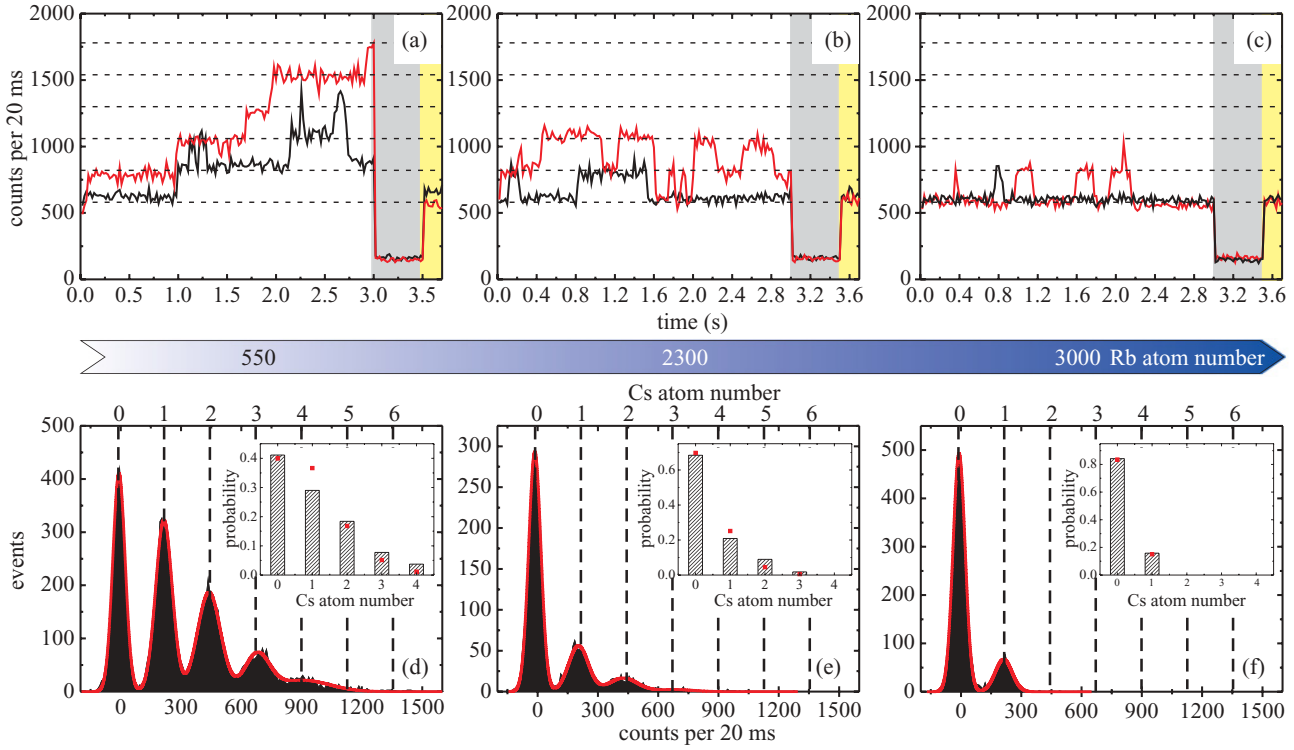

FIG. 2. (Color online) (a)–(c) Typical fluorescence traces of the single-Cs-atom fluorescence signal for a selection of three different Rb atom numbers: The detected pulses are binned in time intervals of 20 ms each. Each panel shows two typical fluorescence traces of single Cs atoms in the presence of about 550, 2300, and 3000 Rb atoms, respectively. Within the gray region the cooling laser light and the magnetic field is switched off. For the last 200 ms (yellow shading) the laser light is switched on again to determine the background light level. The Cs-Cs collision event shown in (a) at 2.5 s is one of the very few observed ones. (d)–(f) Corresponding histograms of the Cs fluorescence signal for the same Rb atom number as in (a)–(c). Each peak corresponds to 0,1,2, . . . , atoms, respectively. The red lines are Gaussian fits to the peaks. We find that, not only in steady state, but for all data sets the probability distribution can be well described by a Poissonian function. The insets compare the measured probability distribution (bars) with a fitted Poissonian distribution (red dots).

equation

$$\frac{dN_{\mathrm{Cs}}}{dt} = R(N_{\mathrm{Rb}}) - \gamma\, N_{\mathrm{Cs}} - \beta_{\mathrm{RbCs}} \int n_{\mathrm{Rb}}(r,t)\, n_{\mathrm{Cs}}(r,t)\, d^3r - \beta_{\mathrm{CsCs}} \int n_{\mathrm{Cs}}^2(r,t)\, d^3r. \quad (1)$$

Here, the first term is the Rb atom-number-dependent loading rate $R(N_{\mathrm{Rb}})$; the second term describes the loss of Cs atoms due to collisions with background gas particles at a rate γ; the third and fourth terms describe, respectively, the loss of Cs atoms due to collisions with a Rb and Cs atom, characterized by the inelastic collision coefficients β_{RbCs} and β_{CsCs}. In our particular system of single Cs atoms, the different terms can be determined either directly by the recorded fluorescence traces or by independent measurements or can be neglected. In contrast to common balanced many-body mixtures, here only the value of the inelastic Rb-Cs collision coefficient β_{RbCs} remains unknown. In the following each term is discussed separately.

The background collision rate γ is determined by an independent measurement in the absence of Rb to be $(0.03 \pm 0.01)\ \mathrm{s}^{-1}$. The last term describing Cs-Cs collisions which rarely occur due to the extremely low Cs density and lead to a simultaneous loss of two Cs atoms can be neglected. This is an important advantage in comparison to balanced many-body mixtures, where intraspecies interactions have to be taken into account.

In order to determine the first term in Eq. (1), we obtain the loading rate of the detected traces by counting the loading steps and averaging over the detection time. This is plotted as a function of the Rb atom number in Fig. 3(a), showing a linear decrease of the loading rate for an increasing number of Rb atoms described by $R(N_{\mathrm{Rb}}) = R_0 - \alpha\, N_{\mathrm{Rb}}$, where R_0 denotes the loading rate of Cs without Rb and α is the proportionality factor. A linear fit determines the parameters to be $R_0 = (1.48 \pm 0.06)\ \mathrm{s}^{-1}$ and $\alpha = (2.3 \pm 0.3) \times 10^{-4}\ \mathrm{s}^{-1}$. We attribute the decreasing loading rate with increasing Rb atom number to the fact that the relatively large Rb MOT operates as a shield for the Cs MOT. The enhanced Rb partial background pressure surrounding the Cs MOT in combination with the MOT laser beams leads to light-induced cold collisions during the capturing process of Cs atoms, thereby reducing the Cs loading rate for an increasing number of Rb atoms stored.

Analogously to the loading rate, the loss counts per time are determined by averaging over the detection time, which is in general different from the loss rate, i.e., the inverse lifetime of an atom in the trap. The time-averaged loss counts, which are plotted in Fig. 3(b), however, do not show a monotonic

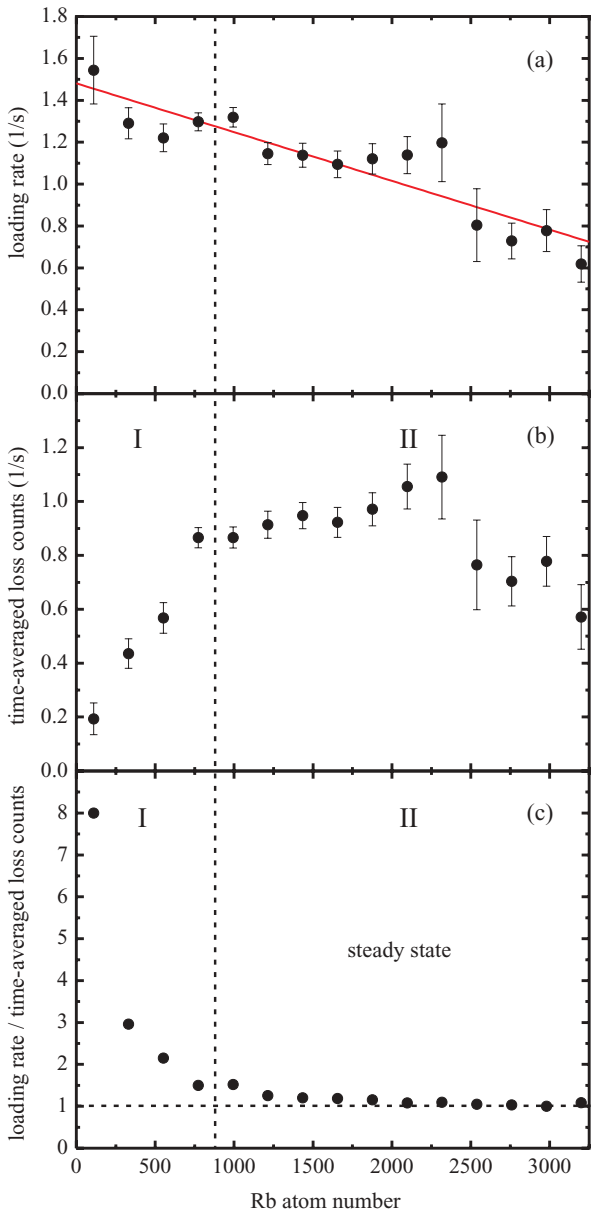

FIG. 3. (Color online) Dynamics of the Cs MOT depending on the number of Rb atoms trapped: (a) Loading rate. The red line is a linear fit to the data yielding $R_0 = (1.48 \pm 0.06)$ s^{-1} and $\alpha = (2.3 \pm 0.3) \cdot 10^{-4}$ s^{-1}. (b) Time-averaged loss counts, and (c) ratio of loading rates and time-averaged loss counts. The vertical dashed line divides the graphs into two sections. Within section I the loading rate dominates the Cs MOT dynamics. For larger Rb atom number (section II) the ratio between loading rates and time-averaged loss counts tends to unity (horizontal dashed line), which corresponds to Cs being in steady state.

behavior, which can be explained by regarding the ratio of the loading rate to the time-averaged loss counts presented in Fig. 3(c). Within the first region (I) for Rb atom numbers of up to 1000, the loss counts per time increase with a rising number of Rb atoms. Here, the loading rate dominates the dynamics of the single-Cs-atom MOT. However, although the loading rate decreases, leading to fewer captured Cs atoms, the loss counts per time is seen to increase. Hence, the enhancement of losses has to be a two-species effect and can be attributed to cold collisions between Cs and Rb discussed in Ref. [1]. In this range of Rb atom numbers, where the loading rate exceeds the value of the time-averaged loss counts, the measured mean Cs atom number depends on the loading and detection time, which can also be seen in the fluorescence traces of Fig. 2(a). The Cs atom number increases continuously over the detection time without reaching a final steady-state value until the MOT is switched off.

For higher Rb atom numbers, i.e., in Sec. II, the ratio between loading rate and loss counts per time tends to unity as shown in Fig. 3(c). Therefore, the evolution of the time-averaged loss counts is determined by the loading rate. Within this section on average each loaded atom leaves the MOT again during the detection time. In this regime the Cs system is in steady state, implying that the average Cs atom number does not change with an increasing loading and detection time.

Thus, for a Rb atom number larger than 1000, the time derivative of the mean Cs atom number $\bar{N}_{\mathrm{Cs}}$ can be set to zero and the steady-state number $\bar{N}_{\mathrm{Cs}}$ of Cs atoms is given by a simplified version of Eq. (1) as

$$\bar{N}_{\mathrm{Cs}} = \frac{R_0 - \alpha N_{\mathrm{Rb}}}{\gamma + \beta_{\mathrm{RbCs}} \frac{N_{\mathrm{Rb}}}{(17\pi)^{3/2} w_{\mathrm{Cs}}^3}}. \tag{2}$$

In addition to the steady-state regime of Cs, here also the Rb atom number is assumed to be time independent. In fact, we have observed no effect of the presence of single or few Cs atoms on the overall state of the Rb cloud with several hundred Rb atoms. However, Rb-Rb cold collisions and collisions with background particles limit the lifetime of the Rb MOT, thereby reducing the Rb atom number. Experimentally the total Rb atom number is maintained by continuously reloading Rb atoms from the atomic beam. Therefore, in Eq. (2) a time-independent Gaussian density distribution of the two clouds is assumed [1]

$$n_i(r,t) = n_i(r) = n_i^0 e^{-\frac{r^2}{w_i^2}}, \tag{3}$$

where w_i is defined as the $1/e$ radius of the cloud of species i, and n_i^0 is the corresponding central density. The mean radius of the Cs cloud is calculated to be $w_{\mathrm{Cs}} = 6.6\ \mu$m following [20] and averaging about all Zeeman states. Here, the magnetic field gradient as well as the laser beam parameters, such as intensity, waist, and detuning, are taken into account. For Rb the size of the cloud is four times larger, mainly due to a larger MOT beam size and a different cooling light detuning. The occupation of all different m_F states results in an uncertainty of 15 % of the absolute value of the size of the clouds.

The steady-state Cs atom number $\bar{N}_{\mathrm{Cs}}$ corresponds to the mean value of Poissonian distributed Cs atom numbers measured for one set of experimental parameters. The resulting expectation values of Cs are plotted versus the number of Rb atoms in Fig. 4. A strong decay of the expectation value with increasing N_{Rb} can be observed. We fit Eq. (2) to the data within the steady-state regime to deduce β_{RbCs} as the only free parameter. Extrapolating the fit to the region below 1000 Rb atoms, where the Cs system is not in steady state, the data and the fit deviate. Here, the equilibrium Cs atom number given by the extrapolation exceeds the measured expectation

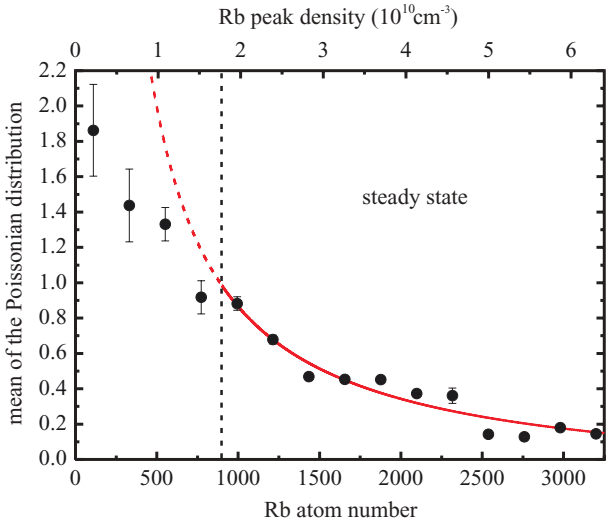

FIG. 4. (Color online) Mean of the Poissonian distribution of Cs atom numbers as a function of the Rb atom number and peak density. The red solid line is a fit of Eq. (2) to the data within the steady-state regime. The red dashed line is the extrapolation to the non-steady-state regime of the Cs MOT.

value, as the measured Cs atom number is limited by the detection time. The inelastic interspecies collision coefficient is determined to be $\beta_{\mathrm{RbCs}} = (1.6 \pm 0.3) \times 10^{-10}$ cm^3/s. The error is given by the statistical uncertainty of the fit. It has been shown [9] that the absolute value of the collision coefficient depends on the laser beam parameters such as intensity and detuning. In principle this can also be investigated by our single-atom method. A systematic deviation of the determined collision coefficient is obtained to be 9×10^{-11} cm^3/s. This value is dominated by the uncertainties of the Rb atom number and the size of the clouds as discussed above. The inelastic interspecies collision coefficient β_{RbCs} includes all mechanisms of inelastic cold collisions summarized as ground-state and light-induced collisions. Our measured value is in good agreement with Rb-Cs collision rate measurements done in a balanced Rb-Cs MOT in Ref. [21] where intra-species interactions cannot be neglected. Our work thereby confirms that a single atom is sufficient to probe large many-body systems.

IV. CONCLUSION

We have illustrated the use of single neutral atoms as a sensitive probe to investigate many-body systems, where the overall state of the many-body system remains unmodified. The inelastic Rb-Cs cold-collision coefficient has been extracted from the dynamics of the single-atom MOT. As a crucial advantage over balanced systems only interspecies interactions have to be considered thereby simplifying the analysis.

This experiment is a step en route toward controlled doping of BECs with impurity atoms as a probe to investigate, e.g., the decoherence of BECs [22] or its phase fluctuations [23]. Since for the presence of near-resonant light it has been shown that the atomic interaction is dominated by light-induced collisions which involve higher electronic states [7–9], a crucial step is to constrain the interaction to coherent ground-state collisions by storing both species in far-off resonant dipole traps. For these species a significant elastic interspecies interaction strength was found [24,25]. In order to investigate the effect of ground-state collisions, time periods involving photon scattering, e.g., preparation or detection, must be temporally and spatially separated from time intervals of ground-state collisions. Here, Feshbach resonances can be exploited to tune the Rb-Cs interaction strength [26] enabling interactions in only preset periods of time.

ACKNOWLEDGMENTS

We thank T. Weikum for contributions to the fluorescence detection system, and W. Alt, O. Fetsch, and A. Moqanaki for helpful discussions. We gratefully acknowledge financial support from the science ministry of North Rhine-Westphalia (NRW MWIFT) through an independent Junior Research Group. N.S. acknowledges support from Studienstiftung des deutschen Volkes and N.S. and C.W. from the Bonn Cologne Graduate School.

[1] A.-C. J. Weiner, V. S. Bagnato, S. Zilio, and P. S. Julienne, Rev. Mod. Phys. **71**, 1 (1999).
[2] M. Taglieber, A.-C. Voigt, F. Henkel, S. Fray, T. W. Hänsch, and K. Dieckmann, Phys. Rev. A **73**, 011402 (2006).
[3] F. M. Spiegelhalder, A. Trenkwalder, D. Naik, G. Kerner, E. Wille, G. Hendl, F. Schreck, and R. Grimm, Phys. Rev. A **81**, 043637 (2010).
[4] A. J. Kerman, J. M. Sage, S. Sainis, Thomas Bergeman, and David DeMille, Phys. Rev. Lett. **92**, 153001 (2004).
[5] S. D. Kraft, P. Staanum, J. Lange, L. Vogel, R. Wester, and M. Weidemüller, J. Phys. B **39**, S993 (2006).
[6] A.-C. Voigt, M. Taglieber, L. Costa, T. Aoki, W. Wieser, T. W. Hänsch, and K. Dieckmann, Phys. Rev. Lett. **102**, 020405 (2009).
[7] S. D. Gensemer, P. L. Gould, P. J. Leo, E. Tiesinga, and C. J. Williams, Phys. Rev. A **62**, 030702 (2000).
[8] A. Gallagher and D. E. Pritchard, Phys. Rev. Lett. **63**, 957 (1989).
[9] D. Sesko, T. Walker, C. Monroe, A. Gallagher, and C. Wieman, Phys. Rev. Lett. **63**, 961 (1989).
[10] M. W. Mancini, A. R.-L. Caires, G. D. Telles, V. S. Bagnato, and L. G. Marcassa, Eur. Phys. J. D **30**, 105 (2004).
[11] It has been pointed out that the heteronuclear loss rates are not reciprocal, i.e., one cannot a priori assume $\beta'_{i,j} = \beta'_{j,i}$.
[12] G. D. Telles, W. Garcia, L. G. Marcassa, V. S. Bagnato, D. Ciampini, M. Fazzi, J. H. Müller, D. Wilkowski, and E. Arimondo, Phys. Rev. A **63**, 033406 (2001).
[13] M. E. Holmes, M. Tscherneck, P. A. Quinto-Su, and N. P. Bigelow, Phys. Rev. A **69**, 063408 (2004).
[14] C. Monroe, W. Swann, H. Robinson, and C. Wieman, Phys. Rev. Lett. **65**, 1571 (1990).
[15] D. Haubrich, H. Schadwinkel, F. Strauch, B. Ueberholz, R. Wynands, and D. Meschede, Europhys. Lett. **34**, 663 (1996).

[16] F. Ruschewitz, D. Bettermann, J. L. Peng, and W. Ertmer, Europhys. Lett. **34**, 651 (1996).

[17] The Geiger mode can be used only for photon rates which are smaller than the inverse dead time of 1/35 ns of the APD. Considering the corresponding detection setups the count rates of Rb and Cs are 10^8/s and 10^5/s, respectively, thus only allowing to operate the Cs APD in the Geiger mode.

[18] For Rb atom numbers less than 700 the statistics is much less, and we average over about 50 traces only. However, this does not influence the analysis of the Rb-Cs interaction parameter, because this is based only on data sets with Rb atom numbers larger than or equal to 1000.

[19] While in steady state the histograms are expected to follow a Poissonian distribution, we find that also for non-steady-state conditions our data are very well described by a Poissonian. For simplicity we therefore fit a Poissonian distribution to the data and extract its mean atom number which is shifted toward smaller values for an increasing number of Rb atoms.

[20] H. J. Metcalf and P. van der Straten, *Laser Cooling and Trapping* (Springer-Verlag, Berlin, 1999).

[21] M. L. Harris, P. Tierney, and S. L. Cornish, J. Phys. B **41**, 035303 (2008).

[22] H. T. Ng and S. Bose, Phys. Rev. A **78**, 023610 (2008).

[23] M. Bruderer and D. Jaksch, New J. Phys. **8**, 87 (2006).

[24] M. Anderlini, E. Courtade, M. Cristiani, D. Cossart, D. Ciampini, C. Sias, O. Morsch, and E. Arimondo, Phys. Rev. A **71**, 061401 (2005).

[25] M. Haas, V. Leung, D. Frese, D. Haubrich, S. John, C. Weber, A. Rauschenbeutel, and D. Meschede, New J. Phys. **9**, 147 (2007).

[26] K. Pilch, A. D. Lange, A. Prantner, G. Kerner, F. Ferlaino, H.-C. Nägerl, and R. Grimm, Phys. Rev. A **79**, 042718 (2009).